High-Order Non-Linear Optical Effects in Organic Luminogens with Aggregation-Induced Emission

Jun Qian, Zhenfeng Zhu, Anjun Qin, Wei Qin, Liliang Chu, Fuhong Cai, Hequn Zhang, Qiong Wu, Rongrong Hu, Ben Zhong Tang, and Sailing He**

Most conventional organic fluorophores are large disc-shaped planar molecules, which tend to aggregate through π–π stacking, and thus suffer from severe aggregation-caused quench (ACQ) effect.[1] Very little or almost no luminescence can be obtained from such organic molecules in their aggregates or the solid state. We have discovered an "abnormal" phenomenon of aggregation-induced emission (AIE),[2] which is diametrically opposite to the ACQ effect. The propeller-shaped AIE molecules are non-emissive in solutions but become highly fluorescent upon the formation of aggregates. Restriction of intramolecular rotations (RIR) has been rationalized as the cause of AIE.[3] Due to the novel effect, one can take advantage of aggregate formation of the luminogens to generate efficient solid emitters (e.g., organic light-emitting diodes (OLEDs)) without complex engineering control,[4] brightly luminescent nanoparticles as bioprobes,[5] sensitive fluorescence turn-on biosensing devices,[6] etc.

Multiphoton absorption/luminescence is a non-linear optical (NLO) process in which several photons are absorbed simultaneously to generate an excited state followed by luminescence processes under certain conditions.[7] In the past two decades, it has been widely applied in bioimaging,[8] photodynamic therapy,[9] frequency-upconverted lasing,[10] 3D microfabrication,[11] 3D optical data storage,[12] and optical stabilization/power limiting.[13] For organic fluorophores, design of long π-conjugated molecular structure is required to achieve large multiphoton absorption cross-section.[7] Previously, some groups have reported some features and applications of two-photon-excited fluorescence of AIE active luminophores in the nanoaggregate state.[14] However, no work has been reported on an organic AIE molecule that exhibits three-/four-photon-excited luminescence (3PL/4PL, a fifth/seventh-order non-linear process) or other NLO effects.

Among the developed AIE luminogens, 2,3-bis(4-(phenyl(4-(1,2,2-triphenylvinyl)phenyl)amino)phenyl)fumaronitrile (TTF) has drawn much attention: it has extended π-conjugation, which makes it possess large multiphoton absorption cross-section and other NLO effects, as well as emit far red/NIR light upon excitation.[15] In the present work, we studied the high-order non-linear optical effects of TTF in three distinct systems, which are monomolecules in organic solution, nanoaggregates in aqueous solution, and in the solid state on a glass slide. In a chloroform/toluene mixture, the 3PL/4PL intensity from TTF molecules gradually enhanced with increasing fraction of toluene under femtosecond (fs) laser excitation, but no other NLO effects could be observed. In TTF nanoaggregates, besides aggregation-induced 3PL enhancement, we also observed third harmonic generation (THG). Excitingly, its intensity was also proportional to the aggregation degree of TTF molecules, which can be named as aggregation-induced THG enhancement. In the solid state of TTF, the 3PL/4PL accompanied by tunable THG and fifth harmonic generation (FHG) signals, could be obtained using a wavelength-tunable femtosecond laser. As application examples, we demonstrate simultaneous multimodal 3PL and THG imaging on tumor cells labeled with TTF-doped-nanoparticles. We also preliminarily applied TTF-doped-nanoparticles in 3PL microscopic in vivo imaging of mouse brains. The unique NLO properties of AIE luminogens based nanoprobes may find potential applications in deep, real-time, and long-time NLO microscopic in vivo imaging.

Figure 1A shows the molecular structure of TTF. It is a typical donor–π–acceptor–π–donor structure, which is helpful to the multiphoton absorption process. The green circled part is π-conjugated, and the groups in the red circle have AIE feature.[15] Absorption spectra of TTF in chloroform and toluene are centered at 515 and 495 nm, respectively (Figure 1B). The red-shift of the absorption maximum of TTF in chloroform was attributed to intramolecular charge transfer (ICT) character,[16]

Prof. J. Qian, Z. Zhu, L. Chu, Dr. F. Cai, H. Zhang, Prof. S. He
State Key Laboratory of Modern Optical Instrumentation, Centre for Optical and Electromagnetic Research, Zhejiang Provincial Key Laboratory for Sensing Technologies, JORCEP (Sino-Swedish Joint Research Center of Photonics)
Zhejiang University
310058 Hangzhou, China
E-mail: sailing@kth.sel

Prof. J. Qian, Q. Wu
Joint Research Laboratory of Optics of Zhejiang Normal University and Zhejiang University
Hangzhou 310058, China

Prof. A. Qin
MoE Key Laboratory of Macromolecular Synthesis and Functionalization
Department of Polymer Science and Engineering, Zhejiang University
Hangzhou 310027, China

Prof. A. Qin, Prof. R. Hu, Prof. B. Z. Tang
SCUT-HKUST Joint Research Laboratory, Guangdong Innovative Research Team, State Key Laboratory of Luminescent Materials and Devices, South China University of Technology (SCUT)
Guangzhou 510640, China
E-mail: tangbenz@ust.hkl

W. Qin, Prof. B. Z. Tang
Department of Chemistry, The Hong Kong University of Science and Technology
Clear Water Bay, Kowloon
Hong Kong, China

DOI: 10.1002/adma.201500141

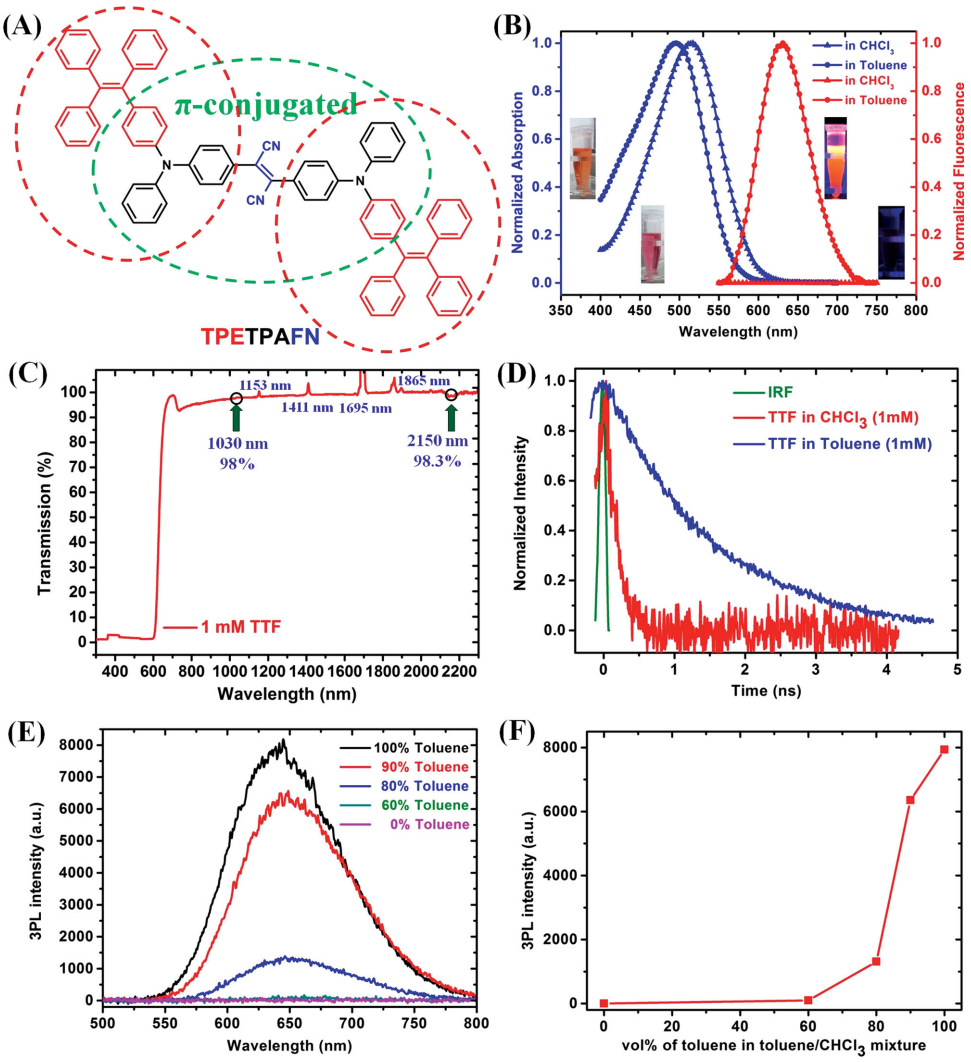

Figure 1. A) Molecular structure of TTF. B) Linear absorption and emission spectra of TTF in chloroform and toluene. Insets: photographs showing chloroform and toluene solution of TTF under visible light (left) and ultraviolet light excitation (right). C) Transmission spectrum of (pure) TTF (1×10^{-3} M, 1 cm thickness). The abnormal spikes around 1153, 1411, 1695, and 1865 nm were attributed to the large linear absorption of chloroform. D) Time-resolved decay profile of 2PL of TTF in chloroform and toluene (excitation laser: 1040 nm, 100 fs, 50 MHz, IRF: 54 ps). E) 3PL from TTF in the chloroform/toluene mixture (1×10^{-3} M, in a glass capillary tube) with various volume ratios of toluene (excited by a femtosecond laser at 1560 nm). F) Variations of 3PL of TTF with volume ratio of toluene in the chloroform/toluene mixture.

since chloroform has higher polarity compared with toluene. TTF has bright fluorescence in toluene, but is almost non-fluorescent in chloroform. It is due to the twisted intramolecular charge transfer (TICT) phenomenon,[17] which is often observed in fluorophores with donor–π–acceptor structure, and featured with red-shifted emission and decreased emission intensity with increasing solvent polarity. As is known, multiphoton absorption occurs at wavelengths where there is no or negligible linear absorption.[7] The transmission spectrum of TTF solution in chloroform (1×10^{-3} M) were measured, by using the transmission spectrum of pure chloroform as the baseline, and the net transmission spectrum of TTF (1×10^{-3} M, with a pass length of 1 cm) was then obtained (Figure 1C). It could be found the transmittance of (pure) TTF molecules in 1030–2300 nm is higher than 98%, and the tiny optical loss in these wavelengths may be attributed to the light scattering by TTF molecules in chloroform, as well as the negligible linear absorption of TTF. Femtosecond lasers in this wide wavelength region can be used to perform the measurement of multiphoton luminescence (MPL) and THG from TTF samples. Two-photon-excited luminescence (2PL) of TTF in the chloroform/toluene mixture and the solid state, under 1040 nm–fs excitation, was shown in Figure S10, Supporting Information. The 2PL lifetime of TTF in chloroform and toluene are estimated (through the time-resolved decay curves shown in Figure 1D) to be 0.2 and 1.5 ns, respectively. The shortening of TTF lifetime in chloroform is also ascribed to TICT phenomenon, which activates non-radiative quenching processes.[17]

In the chloroform/toluene mixture, only 3PL could be observed from TTF, under 1560 nm–fs laser excitation (Figure 1E). In this process, the TTF molecules absorbed three photons simultaneously and the excited TTF was finally relaxed

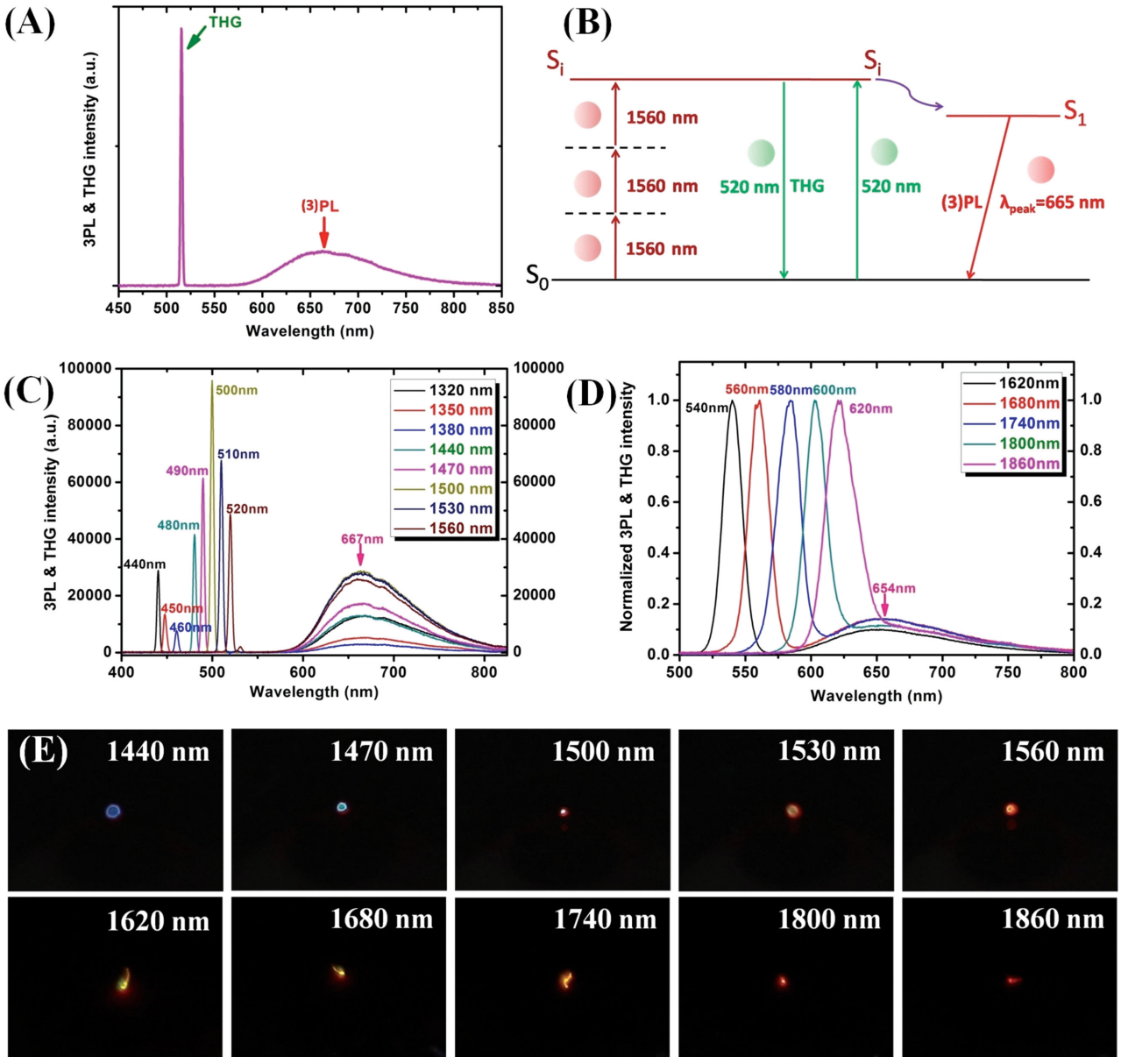

Figure 2. A) Simultaneous 3PL and THG spectra from solid TTF molecules (excited by a femtosecond laser at 1560 nm). B) Diagrams showing the proposed excitation mechanisms of THG and THG-induced 1PL. Optical spectra of coexisted tunable THG and fixed 3PL from solid TTF molecules under femtosecond excitation with various wavelengths [1320–1560 nm in C); 1600–1860 nm in D)]. E) Photographs showing simultaneous tunable THG and fixed 3PL from solid TTF molecules under femtosecond excitation with 1440–1860 nm.

to the lowest excited electronic-vibrational state(s), from which the fluorescence emission occurred. The intensity of 3PL gradually increased, accompanied by blue-shifted peak emission wavelength, with increasing fraction of toluene. The phenomenon was similar to that observed under one-photon excitation (Figure S3, Supporting Information), which was due to TICT character.

Figure 2A shows the simultaneous THG and 3PL spectra from TTF in the solid state, and the intensities of these two kinds of NLO signals are both proportional to the cube of the femtosecond excitation intensity (Figure S12A,B, Supporting Information). Surprisingly, we also found the intensity of 3PL is linearly proportional to the intensity of THG (Figure S12C, Supporting Information). Thus, we suggest an alternative mechanism for the generation of 3PL, namely, the THG photons (direct generation under femtosecond excitation) might be reabsorbed by the solid TTF molecules to produce the fluorescence (Figure 2B). This mechanism is well supported by some control experiments (detailed discussions can be found in the Supporting Information). This may provide a more efficient way to achieve 3PL signals, since direct 3PL is a fifth-order NLO process, while 3PL induced by one-photon excitation of THG is a linear absorption based on a third-order NLO process.[18] For convenience, we still call this "THG-induced fluorescence (or indirectly generated

3PL)" as "3PL" in the following description. Previously, inorganic materials like metallic nanostructures have been proven to have both 3PL and THG effects.[19] 2PL and THG could also be observed from organic crystals.[20] However, no work has been reported that an organic molecule simultaneously exhibits THG and three-photon fluorescence in its aggregated state.

As shown in Figure 2C,D, the THG signal from solid TTF could be tuned from 440 to 620 nm (the inner spot in Figure 2E changes from blue to red) when the femtosecond excitation was changed from 1320 to 1860 nm (1320–1560 nm was from one femtosecond beam with narrow optical spectrum, and 1620–1860 nm was from another femtosecond beam with wide optical spectrum). It indicated that the NLO process occurred in a very wide wavelength range, and a wavelength-tunable (from blue to deep red) organic solid device could be achieved easily here. The spectra of 3PL were almost the same under femtosecond excitation with different wavelengths (the outer spot in Figure 2E is always red). It may be used to fabricate organic frequency-upconverted laser.

We further prepared aqueous suspension of TTF-dots to study the NLO behaviors of TTF in nanoaggregates. Hydrophobic TTF molecules can be easily encapsulated with mDSPE–PEG molecules to form nanodots in aqueous solution.[21] In our experiment, we have used various weight loading ratios [TTF/(TTF + mDSPE–PEG)] of TTF-dots: 9, 14, and 20 wt%. For each sample, the absorbance at peak wavelength was kept the same as 2.17 (**Figure 3**A), by adjusting the amount of AIE-dots added to the sample. In this case, the TTF concentration of each sample could be considered as the same according to Beer's Law. However, the molecular numbers of TTF in each dot, which stands for the aggregation degree of TTF, were different in each sample. As shown in Figure 3B, higher THG and 3PL intensities were observed in the TTF-dots as the loading ratio of TTF increases. The THG (Figure 3F–H) and 3PL (Figure 3C–E) microscopic imaging results demonstrate this tendency more quantitatively. Considering there is no THG signal observed from TTF solution in toluene (Figure 1E and Figure S15, Supporting Information), where the concentration of TTF is higher or the same as that of TTF in the aqueous suspension. We believe the THG from TTF is related to the aggregation degree of TTF, and the "aggregation-induced THG enhancement" feature of TTF makes sense. Furthermore, since the solid-state TTF is a thin sample with TTF molecules aggregated inside at a very high concentration, while the suspension of TTF-dots can be considered as a thick liquid sample with TTF molecules aggregated inside at a certain

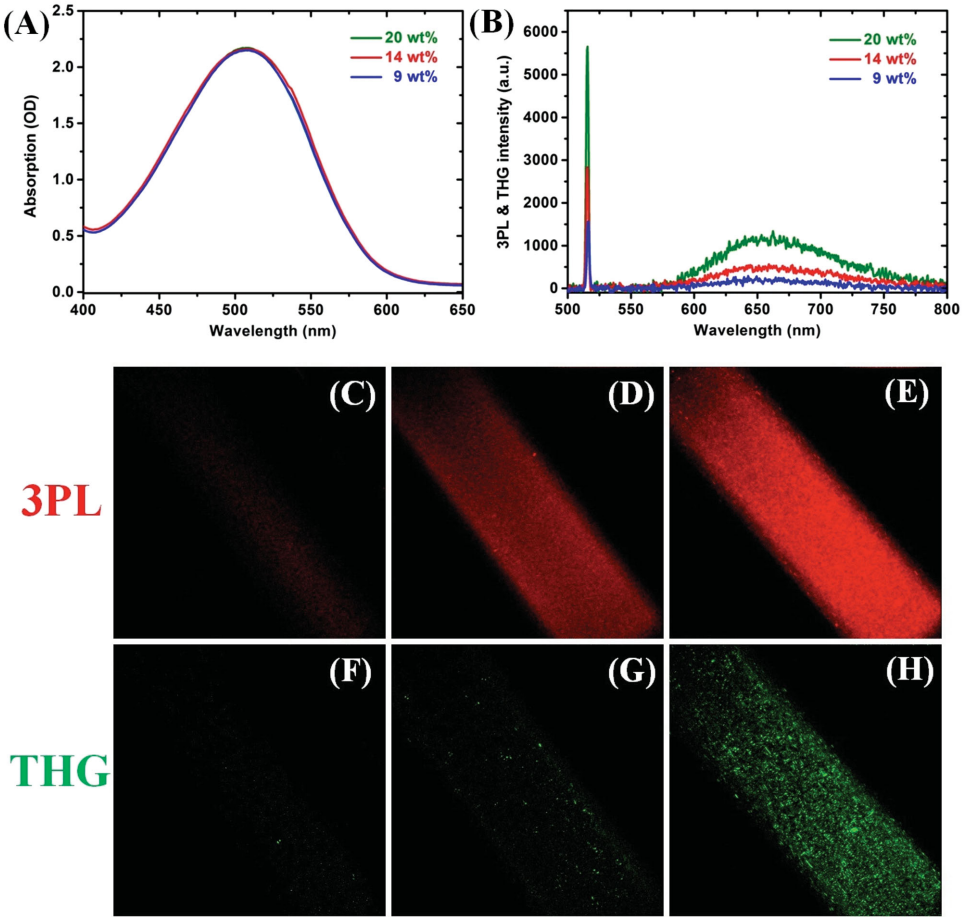

Figure 3. Quantitative comparison of 3PL and THG from AIE-dots with various TTF loading ratios, under the NLO microscope equipped with the 1560 nm–fs laser: Absorption (A) and 3PL&THG (B) spectra of aqueous dispersion of AIE-dots with various TTF loading ratios. 3PL (C–E) and THG (F–H) imaging of aqueous dispersion of AIE-dots in capillary glass tube, with various TTF loading ratios: C,F) 9 wt%, D,G) 14 wt%, E,H) 20 wt%.

concentration, the generation of 3PL of TTF-dots can also be attributed to the re-absorption of the THG photons by the TTF-dots in the dispersion, as the case in the solid state. Thus, the "aggregation-induced 3PL enhancement" may be an integrated result of both "aggregation-induced THG enhancement" and "aggregation-induced enhancement of 1PL."

Compared to ACQ dye, AIE-active TTF can be designed as nanodots with very high doping concentration. Such nanoprobes possessing high linear optical (LO) and NLO emission efficiency, strong photobleaching and photoblinking resistance, as well as excellent biocompatibility, are very suitable for bioimaging.[15,22] Herein, we explored the bioimaging application of nanoaggregated TTF molecules, based on 3PL and THG features. We used TTF-doped-silica nanoparticles[23] (which also possess THG and 3PL under 1560 nm–fs excitation, Figure S16, Supporting Information) to treat tumor cells and performed multimodal NLO imaging. **Figure 4**A shows the 3PL and THG images of HeLa cells (obtained from the ATCC) stained with TTF-doped-nanoparticles. Both the "red" and "green" signals were intense and covered the morphology of cells uniformly. The two images overlap very well, illustrating that both NLO signals were emitted simultaneously from the same nanoprobes. The double-checked

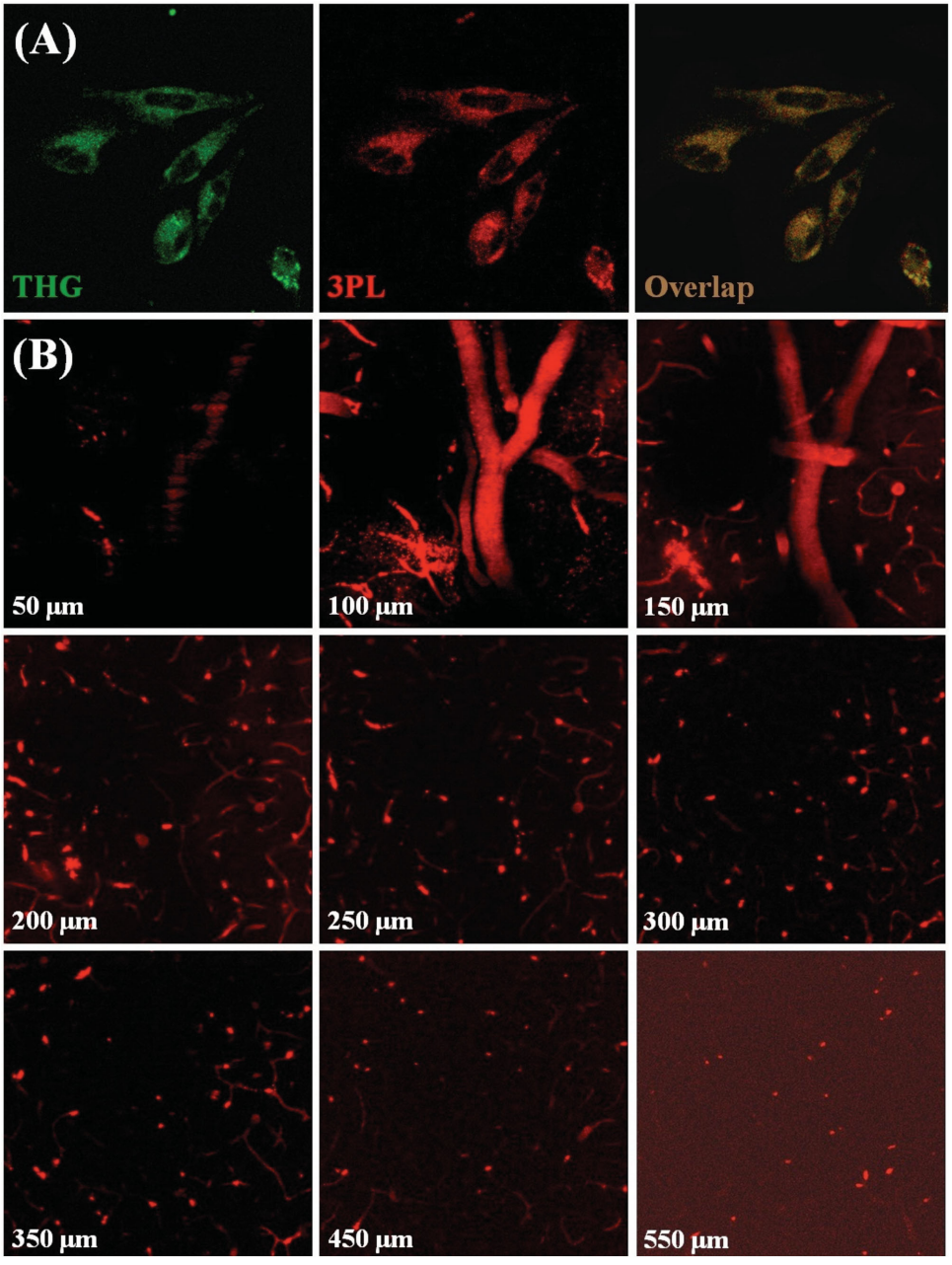

Figure 4. A) 3PL, THG, and their merged microscopic images of HeLa cells, which were treated with TTF-doped-nanoparticles for 2 h. B) 3PL microscopic imaging of brain blood vessels of a mouse (intravenously injected with TTF-dots) at different depths. All the images were taken under the NLO microscope equipped with the 1560 nm–fs laser.

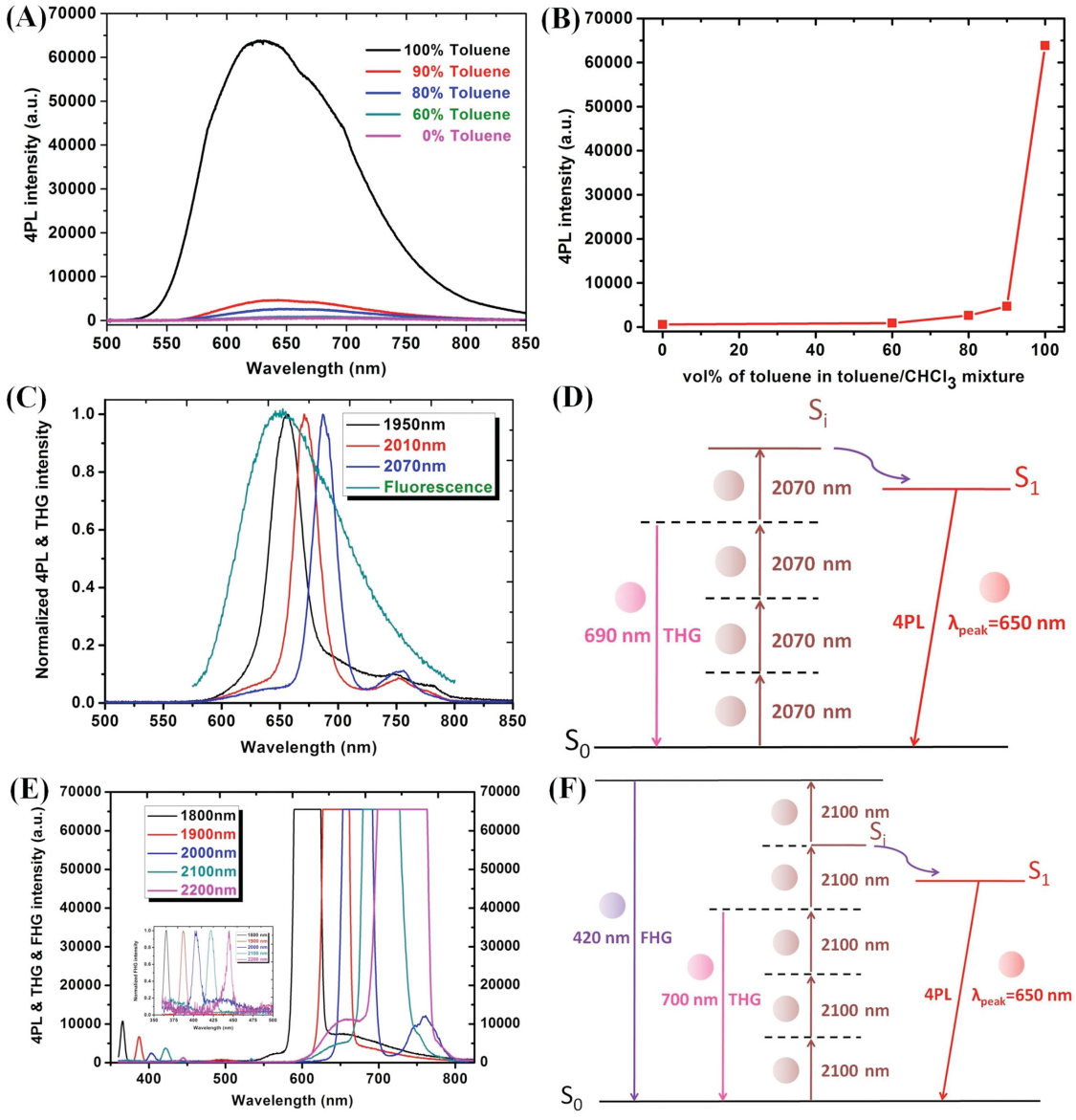

Figure 5. A) 4PL spectra of TTF in the chloroform/toluene mixture (10×10^{-3} M, excited by a 1950 nm–fs laser) with various volume ratios of toluene. B) Variations of 4PL of TTF with volume ratio of toluene in the chloroform/toluene mixture. C) Simultaneous 4PL and THG spectra from solid TTF molecules (excited by a femtosecond laser at 1950, 2010, and 2070 nm, respectively). The peaks centered at about 750 nm were from the background of the excitation fs laser. D) Diagrams showing the proposed excitation mechanisms of 4PL and THG. E) Simultaneous THG, FHG, and 3PL/4PL spectra from solid TTF molecules (excited by a femtosecond laser at 1800, 1900, 2000, 2100, and 2200 nm). Inset: normalized FHG signals. F) Diagrams showing the proposed excitation mechanisms of THG, FHG, and 4PL fluorescence.

NLO signals make the localization of nanoprobes on biosamples more reliable and real-time. Furthermore, we have shown the photobleaching resistance of TTF-doped-silica nanoparticles uptaken by HeLa cells, under three-photon excitation. This is very helpful to some long-term dynamic imaging and observation of bio-samples.

Considering TTF-dots have intense 3PL under 1560 nm femtosecond-excitation, and 1560 nm is very close to an optical tissue window ranging from 1600 to 1800 nm,[24] we tried to apply TTF-dots in 3PL in vivo microscopy imaging. The distinct 3PL from the intravenously injected AIE-dots is helpful to reveal the vascular architecture in the mouse brain at different vertical depth. Some tiny structure of capillary vessels could also be discriminated very clearly. The 3PL imaging depth could reach as deep as 550 μm in the mouse brain. To the best of our knowledge, this is the first report on the utilization of AIE-doped-nanoparticles for 3PL in vivo bioimaging. In the future, if the imaging system is optimized, e.g., tuning the femtosecond–wavelength to the optical tissue window or further compressing the pulse width of femtosecond-excitation, deeper 3PL imaging depth could be achieved, which will be very helpful to many neurophotonics research.

Under 1950 nm–fs laser excitation, only 4PL could be observed from TTF in the chloroform/toluene mixture (**Figure 5**A).

Its intensity is proportional to the fourth power of the femtosecond excitation intensity (Figure S18, Supporting Information). In this process, the TTF molecules directly and simultaneously absorbed four photons and then emitted fluorescence. The intensity of 4PL gradually increased, accompanied by blue-shifted peak emission wavelength, with increasing fraction of toluene (Figure 5B). Figure 5C shows the simultaneous THG and 4PL spectra from solid TTF molecules with femtosecond excitation of 1950, 2010, and 2070 nm. As the THG signals were very intense and overlapped with the spectra of four-photon fluorescence, only partial profiles of fluorescence could be observed. As illustrated in Figure 5D, the total energy of three photons at 2070 nm is not large enough to overcome the bandgap between the ground state (S_0) and excited state (S_1) of TTF. The excited fluorescence was therefore induced by simultaneous absorption of four photons. In other words, since 650, 670, and 690 nm (the same as the peak wavelengths of THG signals with femtosecond excitation of 1950, 2010, and 2070 nm) excitation could not generate 1PL of TTF (Figure S19, Supporting Information), the 4PL of solid TTF molecules should not be induced by the re-absorption of THG. Thus, in this case, THG and 4PL are two independent NLO effects.

Besides THG and MPL, FHG (a fifth-order NLO effect) simultaneously occurred in the solid TTF molecules when the power of the femtosecond laser was further increased. The FHG signal was tunable in the ultraviolet/violet region under fs-excitation from 1800 to 2200 nm (Figure 5E), and the fifth-order NLO effect is also related to the π-conjugation of TTF molecule. Figure 5F is the diagram which describes the three NLO processes (THG, FHG, and 4PL). In the FHG process, TTF molecules absorbed five photons simultaneously. The five photons were then annihilated, and generated a new single photon with five times the frequency. The FHG effect of TTF may be used for ultraviolet/violet organic solid/integrated lasers, as well as high-density optical data storage. The FHG signals may be reabsorbed by the solid TTF molecules and generate 4PL, but its contribution might be very low. 4PL already existed when the fs-excitation power was not very high (no FHG could be observed). Even the FHG was observed when the femtosecond-excitation power increased, its intensity might not be high enough to excite the 1PL of solid TTF molecules.

In summary, we have demonstrated MPL (up to four-photon) of molecular-state TTF in organic solution. Simultaneous 3PL/4PL, THG, and FHG of TTF in the solid state could be observed. In TTF nanoaggregates, we found aggregation-induced THG enhancement and aggregation-induced 3PL. TTF-doped-nanoparticles were further used for multimodal NLO microscopic imaging of tumor cells, as well as 3PL in vivo imaging of mouse brains. The unique NLO effects of AIE fluorogens may find many potential high-tech applications in, for example, biomedical theranostics and photonic devices.

Supporting Information

Supporting Information is available from the Wiley Online Library or from the author.

Acknowledgements

This work was supported by National Basic Research Program of China (973 Program; 2013CB834704 and 2011CB503700), the National Natural Science Foundation of China (61275190 and 91233208), the Program of Zhejiang Leading Team of Science and Technology Innovation (2010R50007), the Fundamental Research Funds for the Central Universities, the Open Fund of the State Key Laboratory of Luminescent Materials and Devices (South China University of Technology), the Swedish Research Council, SOARD, and The Research Grants Council of Hong Kong (HKUST2/CRF/10). The protocols for the animal experiments were approved by the Institutional Ethical Committee of Animal Experimentation of Zhejiang University in China, and the experiments were performed strictly according to governmental and international guidelines on animal experimentation. According to requirements for Biosafety and Animal Ethics, all efforts were made to minimize the number of animals used and their suffering.

Received: January 11, 2015
Published online: February 25, 2015

[1] J. B. Birks, *Photophysics of Aromatic Molecules*, Wiley, London, UK, **1970**.
[2] J. D. Luo, Z. L. Xie, J. W. Y. Lam, L. Cheng, H. Y. Chen, C. F. Qiu, H. S. Kwok, X. W. Zhan, Y. Q. Liu, D. B. Zhu, B. Z. Tang, *Chem. Commun.* **2001**, 1740.
[3] Y. N. Hong, J. W. Y. Lam, B. Z. Tang, *Chem. Commun.* **2009**, 4332.
[4] H. Y. Chen, J. W. Y. Lam, J. D. Luo, Y. L. Ho, B. Z. Tang, D. B. Zhu, M. Wong, H. S. Kwok, *Appl. Phys. Lett.* **2002**, *81*, 574.
[5] a) W. Qin, D. Ding, J. Z. Liu, W. Z. Yuan, Y. Hu, B. Liu, B. Z. Tang, *Adv. Funct. Mater.* **2012**, *22*, 771; b) Q. L. Zhao, K. Li, S. J. Chen, A. J. Qin, D. Ding, S. Zhang, Y. Liu, B. Liu, J. Z. Sun, B. Z. Tang, *J. Mater. Chem.* **2012**, *22*, 15128.
[6] a) Y. N. Hong, M. Haussler, J. W. Y. Lam, Z. Li, K. K. Sin, Y. Q. Dong, H. Tong, J. Z. Liu, A. J. Qin, R. Renneberg, B. Z. Tang, *Chem. Eur. J.* **2008**, *14*, 6428; b) Y. N. Hong, C. Feng, Y. Yu, J. Z. Liu, J. W. Y. Lam, K. Q. Luo, B. Z. Tang, *Anal. Chem.* **2010**, *82*, 7035.
[7] G. S. He, L. S. Tan, Q. Zheng, P. N. Prasad, *Chem. Rev.* **2008**, *108*, 1245.
[8] J. Qian, D. Wang, F. H. Cai, W. Xi, L. Peng, Z. F. Zhu, H. He, M. L. Hu, S. L. He, *Angew. Chem. Int. Ed.* **2012**, *51*, 10570.
[9] a) S. Kim, T. Y. Ohulchanskyy, H. E. Pudavar, R. K. Pandey, P. N. Prasad, *J. Am. Chem. Soc.* **2007**, *129*, 2669; b) J. Qian, D. Wang, F. H. Cai, Q. Q. Zhan, Y. L. Wang, S. L. He, *Biomaterials* **2012**, *33*, 4851.
[10] a) G. S. He, P. P. Markowicz, T. C. Lin, P. N. Prasad, *Nature (London)* **2002**, *415*, 767; b) Q. D. Zheng, H. M. Zhu, S. C. Chen, C. Q. Tang, E. Ma, X. Y. Chen, *Nat. Photonics* **2013**, *7*, 234.
[11] B. H. Cumpston, S. P. Ananthavel, S. Barlow, D. L. Dyer, J. E. Ehrlich, L. L. Erskine, A. A. Heikal, S. M. Kuebler, I. Y. S. Lee, D. McCord-Maughon, J. Q. Qin, H. Rockel, M. Rumi, X. L. Wu, S. R. Marder, J. W. Perry, *Nature (London)* **1999**, *398*, 51.
[12] P. Zijlstra, J. W. M. Chon, M. Gu, *Nature (London)* **2009**, *459*, 410.
[13] a) G. S. He, Q. D. Zheng, C. G. Lu, P. N. Prasad, *IEEE J. Quantum Electron.* **2005**, *41*, 1037; b) G. S. He, K. T. Yong, Q. D. Zheng, Y. Sahoo, A. Baev, A. I. Ryasnyanskiy, P. N. Prasad, *Opt. Express* **2007**, *15*, 12818.
[14] a) S. Kim, H. E. Pudavar, A. Bonoiu, P. N. Prasad, *Adv. Mater.* **2007**, *19*, 3791; b) J. Geng, K. Li, W. Qin, L. Ma, G. G. Gurzadyan, B. Z. Tang, B. Liu, *Small* **2013**, *9*, 2012.
[15] K. Li, W. Qin, D. Ding, N. Tomczak, J. Geng, R. Liu, J. Liu, X. Zhang, H. Liu, B. Liu, B. Z. Tang, *Sci. Rep.* **2013**, *3*, 1150.
[16] M. Maiti, T. Misra, T. Bhattacharya, C. Basu (nee Deb), A. De, S. K. Sarkar, T. Ganguly, *J. Photochem. Photobiol.* **2002**, *152*, 4.

[17] R. R. Hu, E. Lager, J. Z. Liu, J. W. Y. Lam, H. H. Y. Sung, I. D. Williams, Y. C. Zhong, K. S. Wong, P. C. Eduardo, B. Z. Tang, *J. Phys. Chem. C* **2009**, *113*, 15845.
[18] R. W. Boyd, *Nonlinear Optics*, Academic, New York, **2010**.
[19] L. Tong, C. M. Cobley, J. Y. Chen, Y. N. Xia, J. X. Cheng, *Angew. Chem. Int. Ed.* **2010**, *49*, 3485.
[20] Y. Z. Shen, J. Swiatkiewicz, P. Markowicz, P. N. Prasad, *Appl. Phys. Lett.* **2001**, *79*, 2681.
[21] D. Wang, J. Qian, W. Qin, A. J. Qin, B. Z. Tang, S. L. He, *Sci. Rep.* **2014**, *4*, 4279.
[22] D. Wang, J. Qian, S. L. He, J. S. Park, K. S. Lee, S. H. Han, Y. Mu, *Biomaterials* **2011**, *32*, 5880.
[23] H. Cheng, W. Qin, Z. F. Zhu, J. Qian, A. J. Qin, B. Z. Tang, S. L. He, *Prog. Electromagn. Res.* **2013**, *140*, 313.
[24] N. G. Horton, K. Wang, D. Kobat, C. G. Clark, F. W. Wise, C. B. Schaffer, C. Xu, *Nat. Photonics* **2013**, *7*, 205.